Biochimica et Biophysica Acta 1817 (2012) 1177–1190

Contents lists available at SciVerse ScienceDirect

Biochimica et Biophysica Acta

journal homepage: www.elsevier.com/locate/bbabio

Extended protein/water H-bond networks in photosynthetic water oxidation ☆

Ana-Nicoleta Bondar *, Holger Dau **

Free University Berlin, Department of Physics, Arnimallee 14, 14195 Berlin

ARTICLE INFO

Article history:
Received 1 February 2012
Received in revised form 19 March 2012
Accepted 28 March 2012
Available online 4 April 2012

Keywords:
Hydrogen bonding
Oxygen evolution
Photosystem II
Photosynthesis
Proton transfer

ABSTRACT

Oxidation of water molecules in the photosystem II (PSII) protein complex proceeds at the manganese–calcium complex, which is buried deeply in the lumenal part of PSII. Understanding the PSII function requires knowledge of the intricate coupling between the water-oxidation chemistry and the dynamic proton management by the PSII protein matrix. Here we assess the structural basis for long-distance proton transfer in the interior of PSII and for proton management at its surface. Using the recent high-resolution crystal structure of PSII, we investigate prominent hydrogen-bonded networks of the lumenal side of PSII. This analysis leads to the identification of clusters of polar groups and hydrogen-bonded networks consisting of amino acid residues and water molecules. We suggest that long-distance proton transfer and conformational coupling is facilitated by hydrogen-bonded networks that often involve more than one protein subunit. Proton-storing Asp/Glu dyads, such as the D1-E65/D2-E312 dyad connected to a complex water-wire network, may be particularly important for coupling protonation states to the protein conformation. Clusters of carboxylic amino acids could participate in proton management at the lumenal surface of PSII. We propose that rather than having a classical hydrophobic protein interior, the lumenal side of PSII resembles a complex polyelectrolyte with evolutionary optimized hydrogen-bonding networks. This article is part of a Special Issue entitled: Photosynthesis Research for Sustainability: from Natural to Artificial.

1. Introduction

In oxygenic photosynthesis, light-driven water oxidation is facilitated by an astounding protein complex, the photosystem II (PSII), which is embedded in the thylakoid membrane of all cyanobacteria, algae, and terrestrial plants [1–17]. The major subunits (D1, D2, CP43, CP47, PsbO) of the PSII core complex shown in Fig. 1 are evolutionary conserved, whereas several smaller subunits present in the shown cyanobacterial PSII are not found in plants [3,14]. The PSII function as a light-driven water-plastoquinone oxidoreductase is coupled to acidification of the lumen and alkalization of the stroma according to:

$$2H_2O + 2Q + 4Photons \rightarrow 2QH_2 - 4H^+_{Stroma} + 4H^+_{Lumen} + O_2, \quad (1)$$

where Q denotes a plastoquinone molecule (Q_B in Fig. 1). The four protons denoted as H^+_{Lumen} are created by the splitting of two water molecules and released into the inner-thylakoid space, the lumen, which is separated from the stroma by the thylakoid membrane; uptake of the four protons denoted as H^+_{Stroma} results from protonation of reduced plastoquinone molecules. Eq. (1) in conjunction with Fig. 1 indicates that *i*) protons are crucial in the redox chemistry of PSII; *ii*) for each turnover of the reaction cycle, several protons need to be transferred over a distance that exceeds the range of an elementary proton-hopping step (<3 Å). The routes of long-distance transfer of the donor-side protons are addressed herein. Clusters of polar groups and water molecules likely facilitate the long-distance transfer of protons from the oxygen-evolving complex (OEC), the catalytic site of water oxidation, to the periphery of PSII. Clusters of protonatable residues may allow for an efficient transfer of the protons from the water-oxidation site into the aqueous phase. Based on the stunning breakthroughs in protein crystallography on PSII [18,19,2], we will identify and discuss potentially crucial clusters of hydrogen-bonded (H-bonded) residues and water molecules in the lumenal PSII region.

Absorption of a photon by the antenna pigment of PSII initiates a series of electron transfer steps, by which electrons from water (water oxidation) are transferred to a plastoquinone molecule bound at the Q_B-site of PSII [20,21,11]. All key players of the PSII-internal electron transfer chain have been identified and functionally characterized. Recent developments in PSII research support a crucial role of 'smart' proton relocation steps in the PSII redox chemistry [22–29]. The interrelation between local redox transitions and protonation dynamics on various time and length scales has emerged as a key direction for future research on water oxidation by PSII [30–33,8,16].

☆ This article is part of a Special Issue entitled: Photosynthesis Research for Sustainability: from Natural to Artificial.

* Correspondence to: A.-N. Bondar, Free University Berlin, Department of Physics, Theoretical Molecular Biophysics, Arnimallee 14, D-14195 Berlin, Germany. Tel.: +49 30 838 53583; fax: +49 30 838 56510.

** Correspondence to: H. Dau, Free University Berlin, Department of Physics, Biophysics & Photosynthesis, Arnimallee 14, 14195 Berlin, Germany. Tel.: +49 30 838 53581; fax: +49 30 838 56299.

E-mail addresses: nbondar@zedat.fu-berlin.de (A.-N. Bondar), holger.dau@fu-berlin.de (H. Dau).

0005-2728/$ – see front matter © 2012 Elsevier B.V. All rights reserved.
doi:10.1016/j.bbabio.2012.03.031

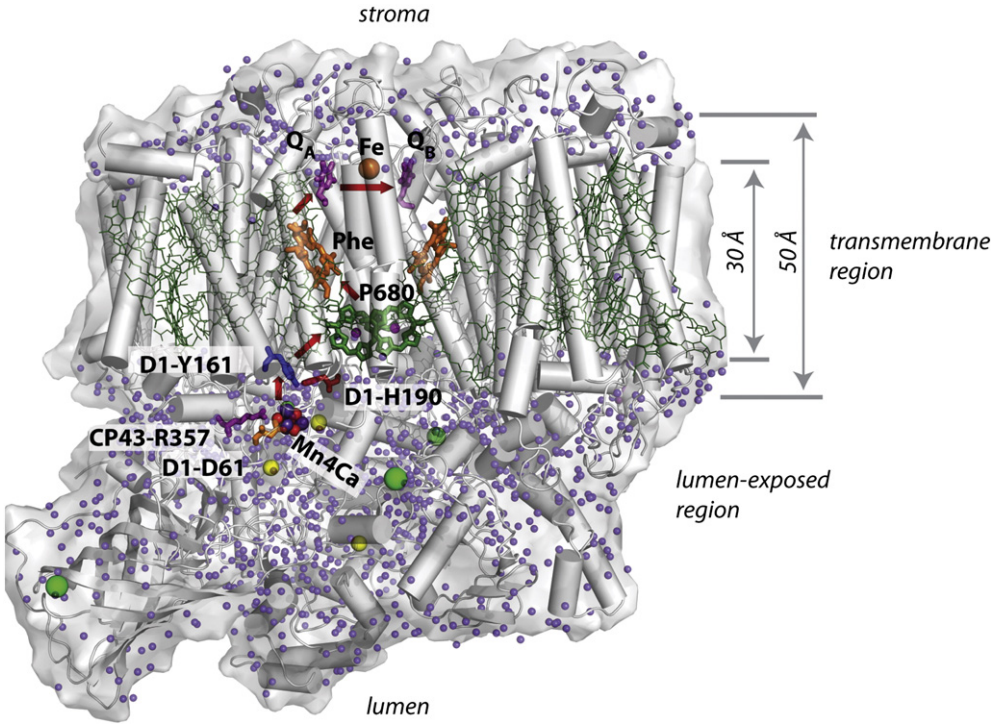

Fig. 1. Schematic representation of the light-driven reactions in PSII. The molecular graphics image was prepared with PyMOL (DeLano Scientific, San Carlos, USA http://www.pymol.org) using the crystal structure from Umena et al. [2]. The red arrows indicate the flow of electrons. See Fig. 2C for a detailed view of crucial residues (D1-61, D1-Y161, and D1-H190).

Water oxidation by PSII takes place at a part of the protein that traditionally is denoted as oxygen-evolving complex (OEC), which comprises a $Mn_4Ca(\mu\text{-}O)_5$ core bound to residues of the D1 and CP43 subunits. (The spatial extension of the OEC is debatable. For simplicity, we will denote the inorganic $Mn_4Ca(\mu\text{-}O)_5$ center as OEC.) There remain uncertainties with respect to the detailed structure of the OEC because of severe X-ray photoreduction (radiation damage) during crystallographic data collection [34–36]; see ref. [7] for a comprehensive evaluation of alternative structural OEC models. The OEC is located close to the interface between the transmembrane and the soluble regions of PSII (Fig. 1). Catalytic water oxidation involves light-induced passage of the OEC through four distinct redox states denoted as S_1, S_2, S_3, and S_0, where the subscript indicates the number of accumulated oxidation equivalents [37,38,25,31]. During one reaction cycle two water molecules are split into four electrons, four protons, and one oxygen molecule (Eq. (1)). Proton removal from the OEC is associated with the transitions $S_0 \rightarrow S_1$ ($1H^+$), $S_2 \rightarrow S_3$ ($1H^+$), and $S_3 \rightarrow S_4$ ($2H^+$) and takes place within tens or hundreds of microseconds (see Junge et al. [39] and refs. therein). The release of protons into the thylakoid lumen contributes to the proton-motive force (PMF) that is used by the cell to synthesize the ATP needed for CO_2 fixation [40,41].

Proton relocation is thought to occur via hydrogen-bonding networks (HBNs) that involve protein groups and water molecules. Proton-transfer channels that may facilitate long-distance proton transfer in PSII have been proposed [19,42,43,32,44,8]. But the relative importance of specific proton transfer networks and the mechanism of transfer remain key open questions. In Section 2, we discuss briefly various views on the long-distance proton transfer in PSII. We then proceed in Sections 3–7 with a new analysis of the HBNs that may facilitate long-distance proton transfer and/or conformational coupling.

In the following, we augment the residue label with the name of the subunit to which the residue belongs. For example, D1-Y161 denotes Y161 of subunit D1 (see, e.g., Fig. 2C). For clarity of the images, the residue labels are color-coded according to the subunit using the color code of Fig. 2D. The four major subunits of the PSII core complex are denoted as D1 (PsbA gene product), D2 (PsbD), CP43 (PsbC), and CP47 (PsbB). The smaller subunits are named according to their gene product. We work exclusively with the crystallographic coordinates of Umena et al. ([2], access code 3ARC, monomer A), where the polypeptide chains are labeled according to the respective gene product (PsbA alias D1 corresponds to chain A, etc.). The PsbV subunit corresponds to the cytochrome c-550, which is present in cyanobacteria but not in the plant PSII, denoted as Cyt-c.

2. Insights by computational studies on PSII proton channels

Regardless of the mechanistic details of how proton transfer is coupled to the electron transfer in the specific S-state transitions, the distance between the OEC and the outer surface of the lumen-exposed region of PSII ($\geq$20 Å) raises the key issue of extended HBNs that may facilitate proton transfer. Indeed, as discussed below, observations from theory and experiments converge towards an image of the protons being released via a dynamic network of channels formed by protein residues and internal water molecules.

The networks of H bonds that could connect the Mn_4Ca cluster to the bulk are rather complex. Since the first specific proton channel was suggested in 2004 [19], no fewer than five putative channels were identified by searching for channels (connected voids) with a minimum diameter of 1.3 Å [46]. The five channels have lengths of about 30–50 Å and a complex architecture. Of the five channels that start close to the Mn_4Ca cluster, two pairs of proton channels unite before reaching the bulk and thus only three channels reach the lumen. D1-E65 (Fig. 2C) was found at the bottleneck of one of the five proton-transfer channels that start close to the Mn_4Ca cluster, and suggested as a possible participant in proton transfer. CP43-R357 (Fig. 2C), a residue previously inferred to deprotonate along with oxidation of the OEC [47], contributes to three of the putative proton-transfer channels identified by Gabdulkhakov et al. [46]. For full listing of the residues contributing to the five putative proton channels, and comparison with paths proposed previously in refs. [43,48], we refer the reader to the discussion in refs. [46,8].

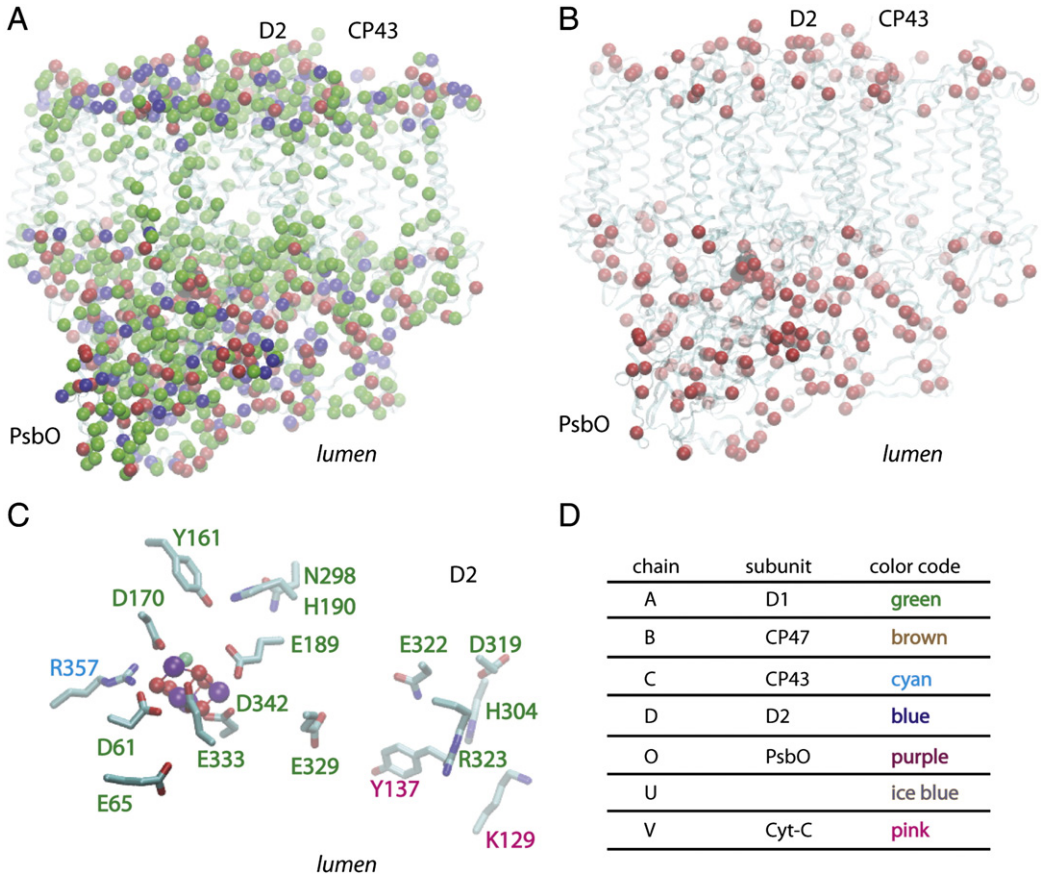

Fig. 2. Polar and charged amino acids in PSII. (A) Cα atoms of the polar and charged sidechains depicted as van-der-Waals spheres. The following colors are used for the Cα atoms: Asp and Glu—red, Arg and Lys—blue, Asn, Gln, His, Ser, Thr, and Tyr—green. A PSII monomer is shown as transparent ribbons. (B) Detailed view of the distribution of the negatively charged groups. Note that the lumen-exposed region of PSII where proton transfer is thought to occur is rich in carboxylic residues. (C) Detailed view of the oxygen-evolving complex (OEC) with the manganese ions shown as violet spheres, oxygen—red, and calcium—green; sidechains of amino acids mentioned in the Introduction are shown as bonds with the carbon atoms colored cyan, nitrogen—blue, and oxygen—red. (D) Color codes used to depict PSII subunits and amino acids that belong to specific subunits. 'Chain' indicates the chain name from the crystal structure of Umena et al. [2], and 'subunit' the standard name of the subunit corresponding to that chain. (The chains are named according to the respective gene products. For example, chain A corresponds to PsbA.) The analysis of HBNs is based on monomer A of the PSII structure from Umena et al. [2]. Molecular graphics images in Figs. 2–10 were prepared using the VMD software [45].

As noted in ref. [46] and ref. [8], dynamics may be important for the PSII channels. Indeed, proteins are dynamic entities, and their dynamics is essential for function [49,50]. Molecular dynamics (MD) simulations are a valuable tool for investigating the dynamics of membrane proteins in hydrated lipid membrane environments at room temperature. To date, long-timescale MD simulations on the complete PSII in a physiological lipid membrane environment have not been performed. Vasil'ev and Bruce [42] reported nanosecond-timescale MD simulations starting from the *T. elongatus* 3.5 Å resolution structure [19]; subunits N, O, U, and V were not included in the MD simulation system. The dynamics of the system was found to affect significantly the calculated rates of electron transfer [42]. A more recent MD simulation starting from the 3.0 Å resolution-structure of the *T. elongatus* PSII and water molecules placed in internal protein cavities [44] revealed that on the 10 ns timescale, the lumen-exposed part of PSII is like a sponge, with an interconnected network of nanopores and numerous water molecules that are highly dynamic and visit multiple sites within the protein. Transient opening and closing of channels was observed during the simulations.

The 1.9 Å resolution structure of the *T. vulcanus* PSII [2] opens new avenues for investigating the proton transfer paths. Umena et al. suggested that D1-Y161 (Fig. 2C) is part of a protein/water H-bonded network that extends far to the lumenal bulk phase [2]. This network, which includes D1 residues H190, N298, N322, R323, D319, and H304, and PsbV K129 and Y137 (Fig. 2C), was suggested as an exit channel for protons [2].

The distance between the OEC and the outer surface of the lumen-exposed region of PSII is large, around 20 Å (Figs. 1, 2A–B, and 3). To travel such long distances, the protons need to 'hop' along H bonds formed by polar protein groups and/or water chains (wires) whose dipoles are suitably oriented (see, e.g., ref. [51]). The large distances that the protons need to travel in PSII, and the complex nature of this multi-subunit protein with numerous inner channels [46,44], raise the intriguing questions of how does the protein ensure efficient movement of protons from the OEC region towards the lumenal bulk. And, to what extent is the protonation state coupled to protein conformation?

Here we contribute to the understanding of the PSII proton channels and long distance coupling between protein subunits by assessing the HBNs. We find extended clusters of protein/water H-bonds. Several of the clusters of H-bonding groups share one or more residues, that is, they are interconnected. Clusters of H bonds can be formed by residues from different subunits of PSII, and extend over significant distances. Four carboxylate dyads that are either buried within PSII, or on the protein surface, are characterized by short, H-bonding distances between the carboxylic groups; such short distances suggest that each of the three carboxylic pairs may harbor a proton.

3. The lumenal region of PSII: a complex polyelectrolyte

Our inspection of the distribution of charged and polar residues in PSII revealed that the lumenal region of the protein is loaded with residues that could H-bond (Fig. 2A). In contrast, the membrane-

intrinsic part of PSII contains a relatively small number of polar groups (mostly histidines), which serve as ligands of the magnesium ions of the PSII chlorophylls.

As expected for a soluble protein [52], PsbO has a large number of residue with polar or charged sidechains (~50%), which are located mostly at the outer side of the partially barrel-shaped protein subunit. We also observe significant polarity in the case of CP43 and CP47: Of the 451 CP43-residues (504 in CP47) in the crystal structure, ~36% (~39% in CP47) are polar or charged (Fig. 2A); given that CP43 (as well as CP47) has six transmembrane (TM) helices, the polarity is higher when calculated for the lumenal region only (44% and 41% of the amino acids in the lumenal regions of CP47 and CP43, respectively, are polar or charged). For comparison, in the case of the largely membrane-embedded D2 subunit (6 TM helices), ~35% (128) of the 342 residues in the crystal structure are polar/charged, with 41% of the lumenal amino acids being polar or charged. The polarity of subunit D2 is relatively close to that of the bacteriorhodopsin proton pump (7 TM helices, 248 residues), which contains ~33% polar/charged groups, with 18 Asp/Glu residues. The values for the D1 subunit are similar (6 TM helices, 335 residues in the crystal structure, 40% polar/charged groups in the lumenal region, of which 13 are Asp/Glu). However unlike bacteriorhodopsin, a protein which translocates proton across the membrane [53], the membrane-spanning subunit of PSII subunits does not contain any Asp/Glu within the transmembrane region (Fig. 2B). Because of the lack of water clusters (Fig. 1) and protonatable residues (Fig. 2A, B), the transmembrane part of PSII cannot allow for proton movements across the thylakoid membrane. In the cytochrome-c oxidase, the redox chemistry is coupled to the translocation of protons across the membrane [54–56]. In PSII, a similar functionality is excluded.

Already mere visual inspection of the high density of water molecules (Figs. 1, 3) and of the remarkable density of polar and charged residues (Fig. 2A, B) reveals that the interior of the lumenal fraction of the PSII proteins cannot be described as a largely hydrophobic protein interior. A coarse discrimination between a hydrophilic protein surface and a hydrophobic protein interior clearly fails. The PSII interior rather resembles a polyelectrolyte brush connected to the membrane-intrinsic (and mostly hydrophobic) region of PSII. Moreover, when turning from the lumenal domain of PSII to the lumen compartment of stacked thylakoid membranes, we find that the volume of the lumen compartment is probably largely filled by the lumenal fraction of PSII proteins [9]. The complete lumen space formed by stacked thylakoids does not form a spacious aqueous bulk phase but rather may resemble a complex polyelectrolyte with aqueous nanometer pores (1–5 nm) between membrane-extrinsic subunits of PSII. The complexity of the situation poses extreme challenges to experimentalists and theoreticians, but ultimately may lead to surprising insights and the development of new and far-reaching concepts.

As opposed to non-biological polyelectrolytes, the distribution of charged residues and water molecules in PSII is not merely statistical but specific enough to become resolvable by protein crystallography. (We note that there are no major voids or other indications that would suggest that a major fraction of water molecules in the protein interior has remained unresolved in the crystal structure of Umena et al. [2].) In protein science (and in biological sciences in general), it often has been a successful strategy to embark on the search for distinctive evolutionary optimized entities (key groups or structural motifs) that could play a crucial role in the function of the macromolecule. Following this strategy and aiming at understanding the protonation dynamics in PSII, first we identify clusters of protonatable residues (Asp/Glu clusters) at the protein surface that may be involved in proton release and/or in the coupling of protonation and conformational dynamics of different PSII subunits at the lumenal surface. Second, we describe 11 prominent HBNs that could participate in the long-distance proton relocation from the OEC to the protein exterior, or in coupling the OEC reactions to remote regions in PSII. Detailed analysis of H-bond patterns led us to identify several intriguing dyads of carboxylic sidechains which likely harbor a proton in the crystallized state and could participate in the dynamic coupling of protonation and conformational dynamics.

In the following, we will discuss three types of HBNs at the lumenal side of PSII: *i*) prominent clusters of carboxylic residues (Asp, Glu) at the PSII surface (SC1–SC12, Figs. 4–6); *ii*) largely protein-internal HBNs of polar amino acid residues and water molecules (HBN1–HBN11, Figs. 7–9); *iii*) two selected surface clusters illustrating special aspects (SC13 and SC14, Fig. 10). Fig. 3 provides an overview of the location of the surface clusters (SCs) and HBNs discussed herein; the connectivity map of Fig. 11 shows schematically the interconnections between the discussed SCs and protein-internal HBNs. The extension and mutual separation of the SCs and HBNs are not uniquely implied by the crystallographic model; clarity of the images and illustration of specific interactions were among the criteria used to select the amino acid residues and water molecules contributing to an individual cluster.

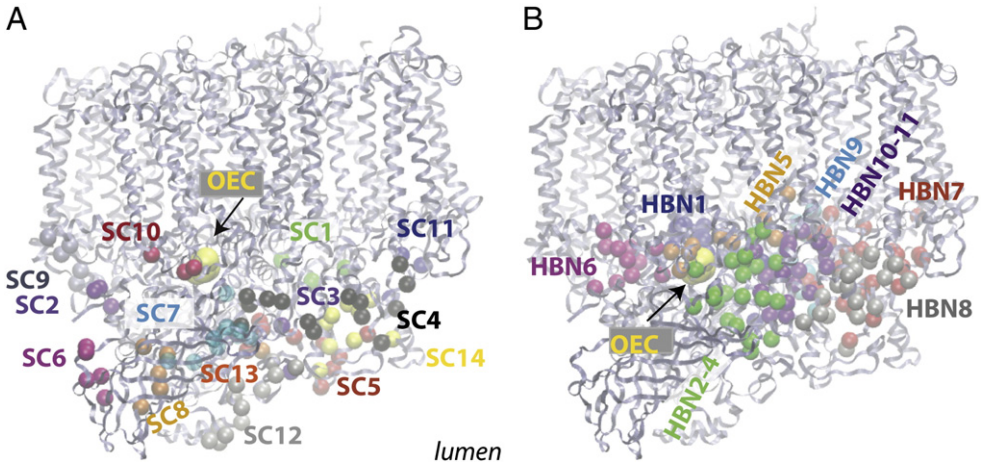

Fig. 3. Location of clusters of amino acid residues discussed in the text. (A) Surface clusters (SC1–SC14) located largely at the surface of PSII. (B) Location of H-bonded networks (HBNs). For simplicity, only the Cα atoms of the cluster-belonging residues are depicted as van-der-Waals spheres. For details about the composition of the clusters, see Fig. 4 (SC1–SC5), Fig. 5 (SC6–SC8), Fig. 6 (SC9–SC12), Fig. 7 (HBN1–HBN4), Fig. 8 (HBN5–HBN6), Fig. 9 (HBN7–HBN11), and Fig. 10 (SC13–SC14). Note that the color codes used to locate the SCs and HBNs are not the same as those used to identify the various protein subunits in Fig. 2D.

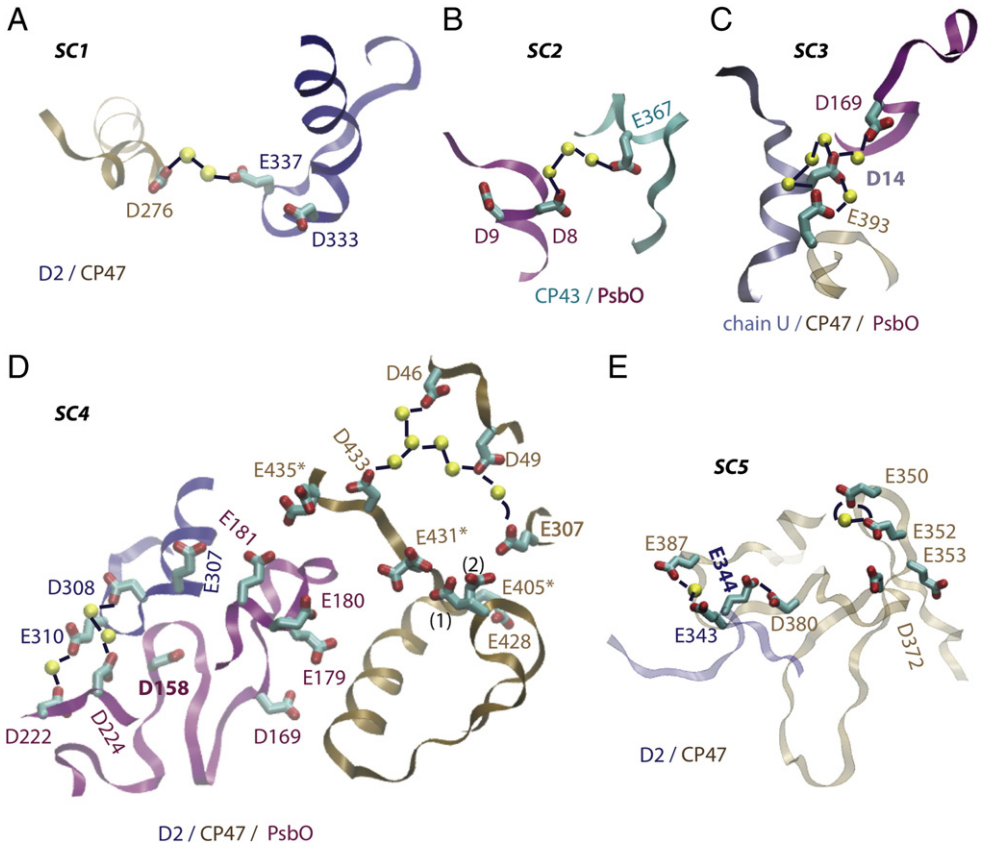

Fig. 4. Inter-subunit carboxylate and carboxylate/water clusters at the lumen-exposed surface of PSII (SC1–SC5). (A–D) Selected carboxylic amino acid sidechains are shown as bonds with carbon atoms colored in cyan and oxygen in red. Here and in all remaining images, each amino acid label is colored according to the PSII subunit to which the amino acid belongs (see Fig. 2D). The straight black lines indicate H-bonding distances (distances ≤ 3.5 Å). The curved lines (e.g., between E350 and E352 in panel E) indicate distances that are somewhat too long for an H bond (between 3.5 Å and 4 Å), but could shorten to H-bonding distances during protein dynamics. Water molecules that bridge Asp/Glu amino acids are depicted as small yellow spheres. In panel E, the distance between D1-E344 and CP47-D380 is 2.6 Å (Table 1), suggesting that a proton is shared by the two carboxylates. The '*' signs in panel D indicate sidechains that have two conformations in the crystal structure. Conformations (1) and (2) of the CP47-E405 sidechain are distinguished by the H-bonding interactions (see text). We note that the definition of the clusters is not unique; the clusters of Asp/Glu groups are defined based on the amino acids being relatively close in terms of distances or sequence, but also to allow an optimal illustration of the interactions.

4. Remarkable carboxylate clusters at the protein surface

4.1. Asp/Glu surface clusters forming H-bonded networks with surface water molecules

Thorough inspection of the Asp/Glu residues on the lumen-exposed surface revealed several remarkable clusters of carboxylic residues located largely on the surface (clusters SC1–SC12, Figs. 3A, 4–6). In these clusters carboxylate sidechains are found at relatively close distances from each other, even within direct H-bonding distance (Fig. 4E). Surface carboxylate groups also participate in networks of protein/water H-bonds (Figs. 4, 5D, 6A–B). The carboxylate/water networks may involve a single water molecule that bridges two carboxylates, for example, the water molecules that bridge D2-E310 to PsbO-D222 in Fig. 4D, and D2-E343 to CP47-E387 in Fig. 4E. Other carboxylate/water networks are more extended, for example, the three-carboxylate/five-water cluster in Fig. 4C, or the network that extends from CP47-E307 to CP47-E433 via five water molecules and two additional Asp groups (Fig. 4D). Since only water molecules that have high occupancy are identified by protein crystallography, it is likely that in physiologic conditions the surface Asp/Glu clusters involve numerous dynamic H bonds between the carboxylates and water molecules of the aqueous bulk. That is, we suggest that each carboxylate cluster corresponds to a dynamic HBN. In what follows, we discuss briefly the carboxylate and carboxylate/water clusters found at the interface between two or three protein subunits, or along the surface of a single protein subunit.

4.2. Inter-subunit Asp/Glu surface clusters

Subunit D2 is connected to CP47 and PsbO via H bonds of carboxylic groups, with (Fig. 4A, D and E) or without (Fig. 4E) intervening water molecules. Particularly strong connections are observed between D2 and CP47 in the region of D2-E343 and D2-E344: the carboxyl group of D2-E344 is within 2.6 Å distance from CP47-D380, and D2-E343 bridges to CP47-E387 via a water molecule (Fig. 4E). Seven amino acids downstream the D2 sequence, E377 connects to CP47-D276 via two ordered water molecules (Fig. 4A). D2-E308 and E310 are part of a HBN with water molecules and PsbO groups (Fig. 4D). This network of H bonds is close to PsbO-D158 (Figs. 4D and 5A), a conserved amino acid residue whose mutation impairs oxygen evolution and chloride retention, albeit the mutant PsbO still binds to PSII [58]. The proximity between PsbO D158 and D228 (the distance between the carboxylic groups of these two aspartates is ~7 Å) suggests that mutation of D158 could affect the dynamics of H-bonding at the PsbO/D2 interface illustrated in Fig. 4D. We note that such extended perturbations would complicate the interpretation of the molecular origin of the site-directed mutagenesis experiments.

The HBN extending from CP47-E307 to CP47-D433 via CP47-D46/D49 and six water molecules (Fig. 4D) is intriguing, because CP47-E307 and CP47-D433 are in the vicinity of three Glu groups (CP47 E405, E431, and E435) for which the crystal structure indicates two possible conformations. In the conformation labeled (1), the carboxylic group of CP47-E405 is within close distance from that of CP47-E431 regardless of the E431 conformation (distances between the carboxylic oxygen atoms of 2.6–

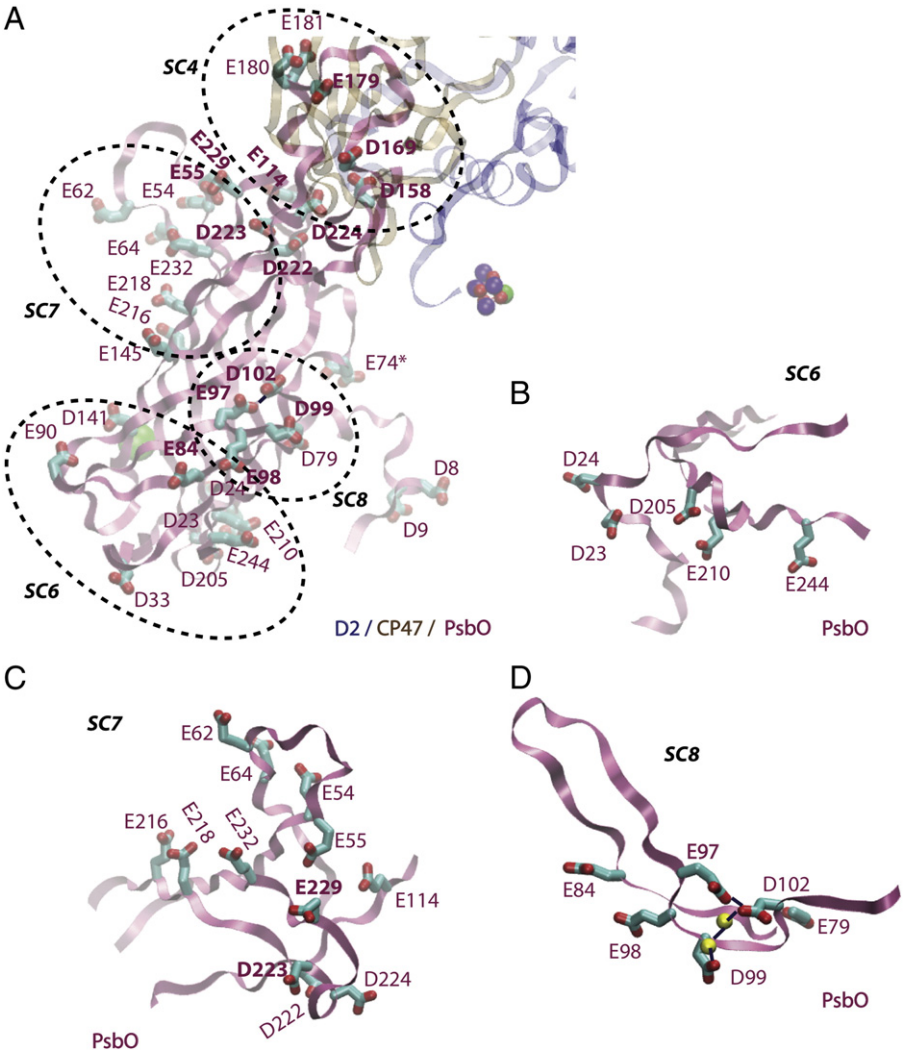

Fig. 5. Carboxylate and carboxylate/water clusters of PsbO (SC6–SC8). (A) Distribution of the PsbO Asp/Glu amino acid residues. PsbO is shown as purple ribbons, with D2 and CP47 in blue and brown, respectively. All sidechains shown explicitly belong to PsbO; for details of carboxylate clusters comprised of PsbO, D2, and CP47 groups, see SC4 in Fig. 4D. Panels B, C, and D show SC6, SC7, and SC8, respectively. The OEC is shown with the oxygen atoms—small red spheres, manganese—violet, and calcium—green. The calcium ion bound to the PsbO surface is shown as a green van-der-Waals sphere. Albeit in panel A the D141 group appears close to the PsbO-bound calcium ion, this amino acid is not part of the calcium coordination shell; the PsbO-bound calcium ion is coordinated by the carbonyl groups of PsbO T138 and V201, and by the N201 sidechain (not shown). In panel D, the distance between the carboxylic sidechains of E97 and D102 is 2.8 Å. We note that surface carboxylate clusters have also been identified by Shutova et al. in the *T. elongatus* PsbO structure [57]. (The PsbO Asp/Glu groups are conserved in *T. elongatus* and *T. vulcanus*.) The *T. elongatus* Asp/Glu discussed by Shutova et al. [57] are E54, E55, E62, E64, D158, D169, E179, E180, E181, D223, D224, E229, and E232. These amino acids overlap with the cluster denoted here as SC7 (Fig. 5C), and with the Asp/Glu at the interface between PsbO and subunits D2/CP47 (Fig. 7A, 9).

3.7 Å, see Table 1). In conformation (2), CP47-E405 is H-bonded to neither E431 nor E307 (Fig. 4D). Likewise, only one of the conformations of the CP47-E435 sidechain is associated with water H-bonding (Fig. 9B). Pursuant to these observations, we suggest that the region close to CP47 E405–E435 is especially dynamic, with a complex pattern of the H-bond dynamics.

4.3. Asp/Glu clusters on the surface of PsbO

The surface of PsbO is rich in carboxylate clusters (see clusters SC4 and SC6–SC8 in Figs. 4D and 5). Most of these Asp/Glu groups are not H-bonded in the crystal structure; exceptions are D97, D99, and D102, which participate in an H-bonded network (cluster SC8, Fig. 5D). The carboxylate groups of E97 and D102 are within 2.8 Å distance (Table 1, Fig. 5D). Such a short distance suggests that one of the carboxylates is protonated, at least in the crystalline PSII.

The observation that in the absence of PsbO, PSII is functional (albeit with different functional properties) [59,3] could be interpreted as evidence that the carboxylate clusters on the surface of PsbO are of low importance for PSII function. We believe that this conjecture would be premature. The insight in the function of PSII in the absence of the PsbO subunit is still limited and does not exclude that the carboxylate clusters directly contribute to optimizing the efficiency of PSII water oxidation. Indeed, it had been indicated that one or more Glu groups of PsbO could be involved in a conformation-coupled proton transfer processes [60,61]. Based on a previous analysis of clusters of carboxylic amino acids from the *T. elongatus* PSII [19], Shutova et al. [57] proposed that closely spaced carboxylates could explain the relatively high pK_a values of PsbO Asp/Glu groups thought to deprotonate during the $S_1 \rightarrow S_2$ transition [60], and that clusters of negatively-charged groups on the surface of PsbO could act as a proton-collecting antenna (see the legend of Fig. 5 for a list of the 13 Asp/Glu amino acids discussed by Shutova et al. [57]). Protonation/deprotonation reactions of surface

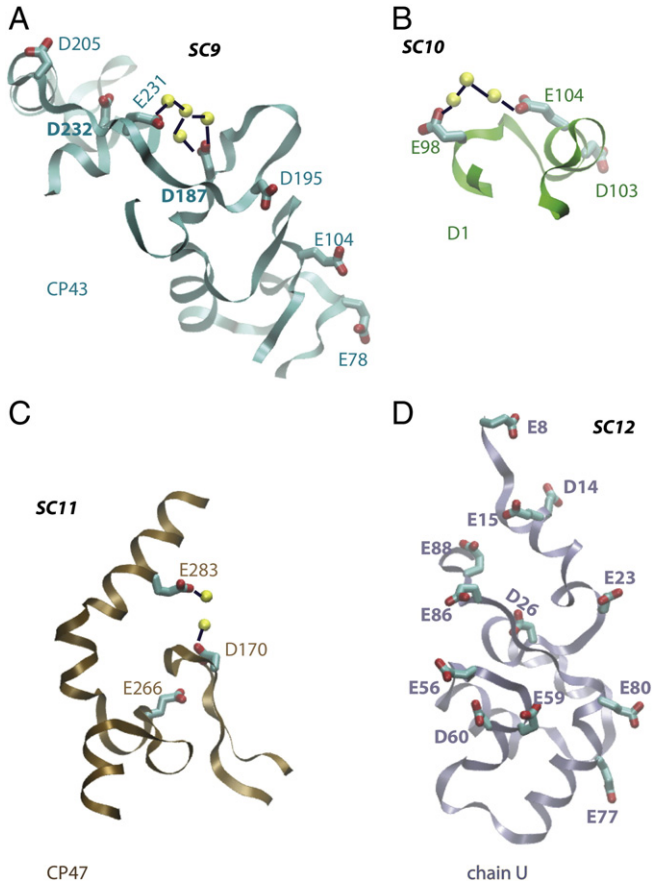

Fig. 6. Carboxylates and carboxylate/water clusters in subunits CP43, D1, CP47, and PsbU (SC9–SC12). The atom colors used are the same as in Fig. 4. In panel C, the distance of 5.3 Å between the two water molecules (yellow spheres) is too large for an H-bond.

carboxylic amino acids may also explain the observed pH-dependent conformational changes of PsbO [62,57]).

4.4. Asp/Glu clusters on the surface of other PSII subunits

We observed clusters of carboxylates on the surface of other PSII subunits, such as CP43 (SC9, Fig. 6A), D1 (SC10, Fig. 6B), CP47 (SC11, Fig. 6C), or chain U (SC12, Fig. 6D). In the case of CP43 and D1, pairs of Asp/Glu groups are bridged via ordered water molecules (Fig. 6A and B). The carboxylate groups of CP47-D170 and E283 are within ~7 Å distance; although the ~5 Å distance between the two water molecules shown in Fig. 6C is too long for a H-bond, we suggest that transient H-bond bridging of CP47-D170 and E283 via water molecules is possible in a physiological environment. The term 'physiological environment' is used here to indicate a non-crystalline PSII embedded in a fluid lipid membrane, surrounded by an aqueous electrolyte; in a physiological environment at room temperature, PSII is a dynamic entity.

The soluble chain U has several Asp/Glu that are closely spaced within the protein sequence, between one and three amino acid residues apart: D14/E15, E23/D26, E56/E59/D60, E77/E80, and E86/E88 (SC12, Fig. 6D). The exact functional role of PsbU is unclear. We speculate that the negative charges of the closely spaced carboxylates discussed here may be involved in the modulation of the PSII affinity for calcium and chloride by the PsbU subunit suggested in ref. [59].

4.5. Possible functional role of the surface carboxylate clusters

Clusters of carboxylates have been observed before on the surface of other proton-transfer proteins—for example, bacteriorhodopsin and cytochrome c oxidase [63,64]. It was proposed that merging of Coulomb cages by closely spaced carboxylates (~8 Å) could ensure a high efficiency of proton exchange [64]. That is, surface carboxylates can act as a proton-collecting antenna [63,65] (or at the lumenal side of PSII, a proton-emitting antenna). MD simulations on the ribosomal S6 protein, a globular protein with approximately 30% of amino acid residues charged at physiological pH, indicated that specific regions on the protein surface function as local ion attractor sites where ions are retained for hundreds of picoseconds; shuttling of ions between nearby attractor sites was also observed [66]. In bacteriorhodopsin, a cluster of carboxylates on the cytoplasmic side of the protein acts as a proton-collecting antenna that assists the passage of the proton from the bulk to the proton-transfer channel [67].

In conclusion, the PSII carboxylate clusters may promote efficient removal of protons from the PSII interior, transient storage of protons, efficient hydration of protons (proton transfer to water molecules of the aqueous bulk), and transfer of the lumenal protons to the ATPase. Moreover, it is conceivable that surface carboxylate clusters, in particular those at subunit interfaces, are involved in controlling protein structure and dynamics.

5. Proton-carrying carboxylate dyads

5.1. H-bonded carboxylate pairs

The short distances between E97 and D102 of PsbO (2.8 Å; Fig. 5D, Table 1) and between D2-E344 and CP47-D380 (2.6 Å, Fig. 4E) are raising the intriguing possibility that the two adjacent carboxylate groups are connected by a strong H-bond, or may even share a proton. The short distance between the carboxylic oxygen appears incompatible with the electrostatic repulsion between two negatively-charged carboxylates. The proton may be shared in the form of a strong, barrierless hydrogen bond without preferential binding to one of the two oxygen atoms ($C_{D/E}-O\bullet\bullet H\bullet\bullet O-C_{D/E}$), or it may be localized at one of the H-bond partners ($C_{D/E}-O-H\cdots O-C_{D/E}$). However, a short H-bonding distance between two carboxylic amino acids in the crystal structure is not sufficient to conclude on whether or not the carboxylic dyads listed in Table 1 carry a proton in the physiological state of PSII. Spectroscopic experiments, pK_a computations, and analysis of H-bond dynamics from prolonged MD simulations would be necessary to further evaluate the protonation states of the dyads and their dynamic changes.

5.2. H-bonded carboxylate pairs in other bioenergetic proteins

Our proposal that the pairs PsbO E97/D102 and D2-E344/CP47-D380 likely have a protonated Asp/Glu is supported by similar observations in other proteins. Short H-bonding distances between Asp/Glu sidechains have indeed been associated with protonated Asp/Glu—for example, in the Na/K pump [68] and in the bacteriorhodopsin proton pump [69,70]. It was noted that in the crystal structures of the Na/K pump [71,72], the distance between the carboxylic groups of E786 and D811 is 2.7–2.8 Å [68]; detailed computational work supplemented by experimental observations led to the conclusion that E786 indeed is protonated [68].

The short-distance Glu dyad interacting with water in PSII resembles the observation that in the proton release site of resting-state bacteriorhodopsin, E194 and E204 are within H-bonding distance (3.0 Å in the structure from ref. [73]), and water molecules are present close to the E194/E204 dyad. The interpretation of this structural arrangement and its associated spectral fingerprints, in terms of a proton storage site, has been controversial (see, e.g., refs. [74–80,69,70]). Based on the crystal structure and interpretation of spectral fingerprints, it was proposed that the proton is stored on the E194/E204 dyad, probably involving also neighboring water molecules [76,77]. Other spectroscopy data were interpreted to suggest E204 as the group from which the proton is released to the bulk [74], or first to E194 [75,81]. The presence of a broad continuum band in the infrared spectrum was proposed to indicate that

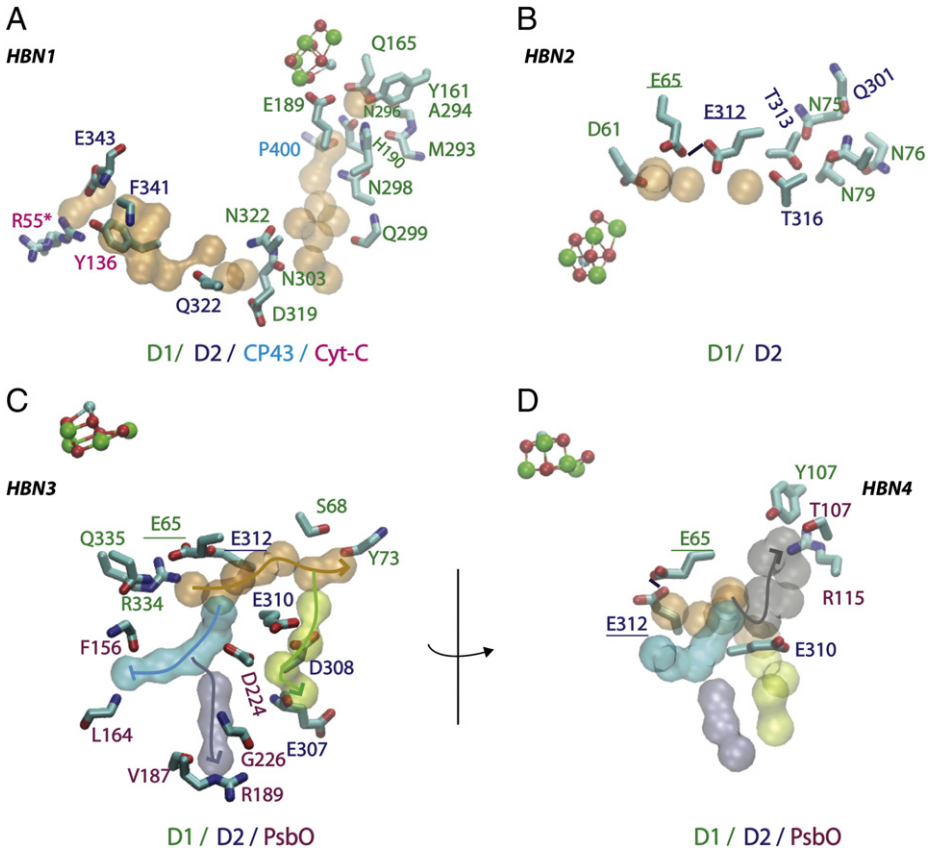

Fig. 7. HBNs and putative pathways for long-distance proton transfer (HBN1–HBN4). The panels illustrate selected HBNs that stem from the vicinity of the OEC. The chloride ion, manganese ions, and oxygen atoms of the OEC are shown, respectively, as cyan, green, and red spheres. Amino acid residues are shown as bonds, and water molecules as transparent surfaces with a probe radius of 1.4 Å. That is, a continuous surface indicates water molecules within H-bonding distance. The PSII subunits contributing to the HBNs are indicated for each panel, e.g., in panel A, the contributing subunits are D1, D2, CP43, and Cyt-c. (A) Curved HBN that extends from the OEC to the solvent-exposed region of Cyt-c. Note that R55* of Cyt-c has two conformations, which suggests an enhanced flexibility in this region of the network. For additional information about the D1-E343 interactions, see Fig. 4E. (B–D) HBNs involving D1-E65 and D2-E312. The black line that connects the carboxyl groups of these two amino acids indicates the 2.5 Å distance between the carboxylic oxygen atoms. Such a short distance could be explained by the two Glu sidechains sharing a proton; the D1-E65/D2-E312 dyad may be a proton-storage site. In panels C and D, the water molecules are colored according to the wires to which they belong. In panel C, four water wires are shown in orange, cyan, ice blue, and dark yellow transparent van-der-Waals spheres; a fifth water wire, colored gray, is depicted in panel D. The curved arrows through the water wires indicate wires that could be part of a pathway for proton release. In contrast, the water wire colored cyan (panel C) leads to non-protonatable backbone groups; although such paths may not participate in proton transfer, they could couple changes in the HBN to structural changes of the backbone. The underlined amino acids are part multiple HBNs (for example, D1-E65 and D2-E312 are part of HBN2–HBN4).

the proton is rather delocalized in a cluster of internal water molecules surrounded by protein residues, including E194 and E204 [79]. The intrinsic proton affinity of a carboxylic group is, however, significantly higher than that of a water dimer, and the crystal-structure geometry is maintained in combined quantum mechanical/molecular mechanical computations with E204 protonated [69]. Recent computations of pK_a values and spectral fingerprints demonstrated that a model in which the proton is shared by E194 and E204 leads to results qualitatively consistent with the experiments [70].

The above summary on the E194/E204 dyad in bacteriorhodopsin illustrates both the need to address the functional role of H-bonded carboxylate groups, and the challenges in assigning protonation

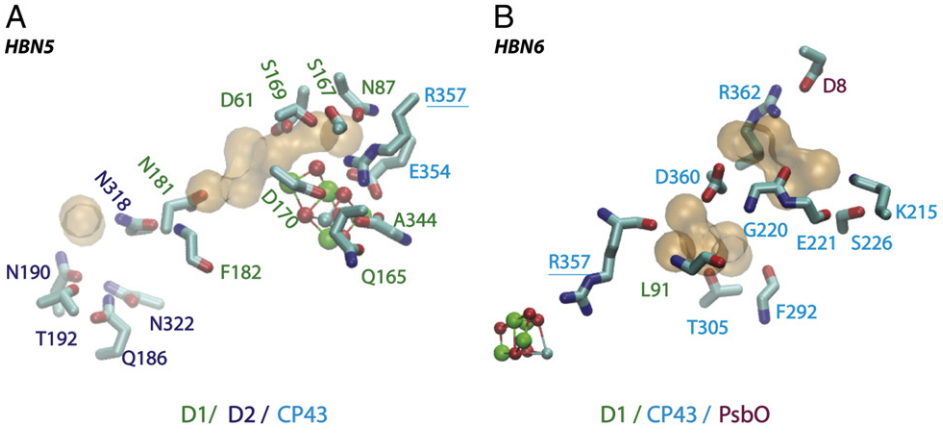

Fig. 8. HBNs close to CP43-R357 (HBN5–HBN6). (A) The CP43-R357 side-chain contributes to an HBN that leads to a cluster of D1 Thr, Asn, and Gln amino acids. (B) The CP43 backbone contributes to a HBN that extends, via CP43-D360, to D8 of PsbO and the aqueous bulk.

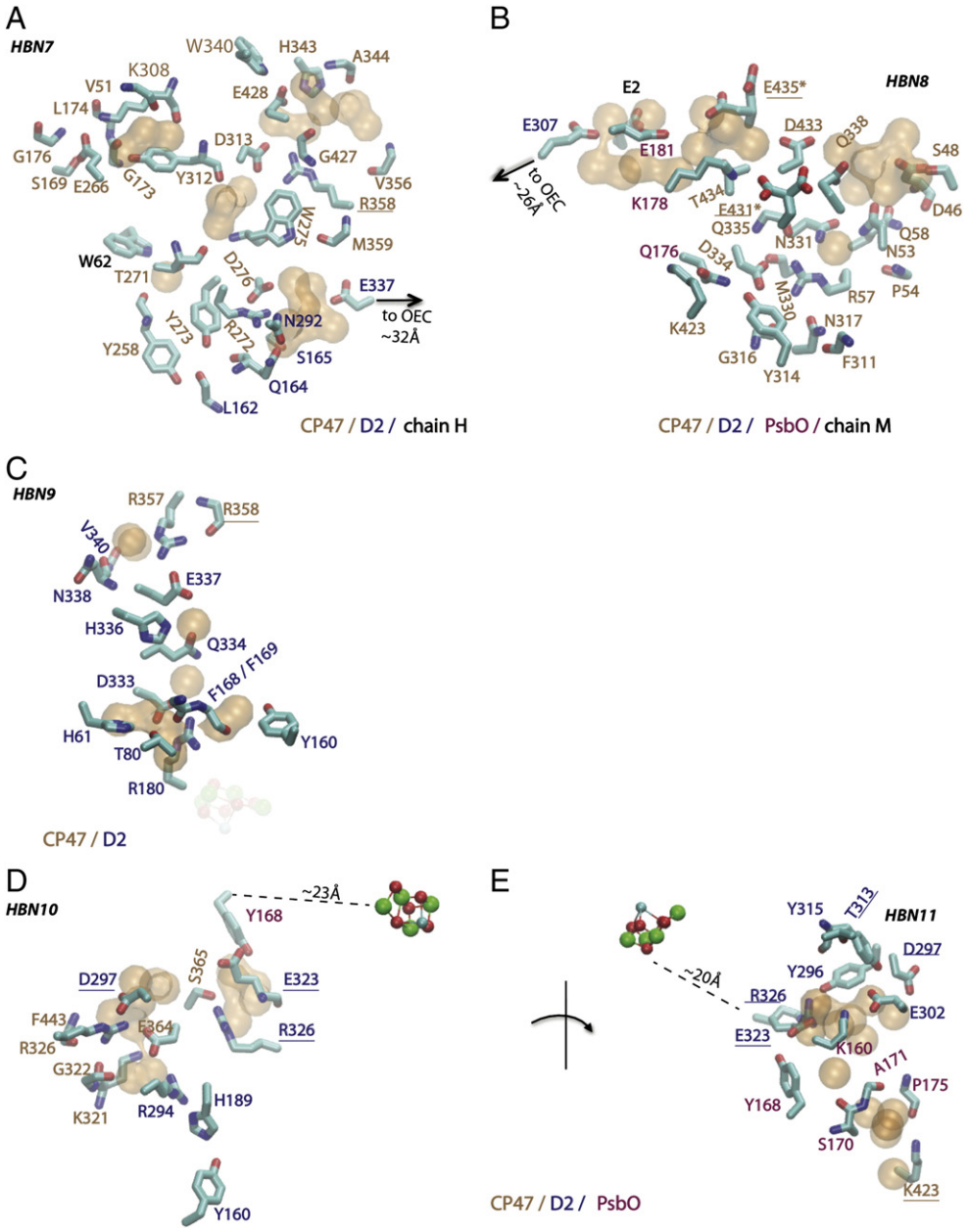

Fig. 9. HBNs located further away from the OEC (HBN7–HBN11). The approximate distance to the OEC is indicated in panels A–B, and D–E. In panel C, the distance between D2-N338 and the OEC is ~33 Å. CP47-R358 contributes to the both HBN7 (panel A) and HBN9 (panel C). Note that D2-D297, E323, and E326 contribute to the both HBN10 (panel D) and HBN11 (panel E); D2-T313 (HBN11, panel E) is also part of HBN2 (Fig. 7B). In panel B, CP47-D433 connects the two halves of HBN8, the CP47-E435 side and the CP47-Q338 side. See Fig. 4D (SC4) for additional information on the region close to the CP47/E431/D433/E435 region. Chains H and M contribute only a single amino acid residue each to HBN7 and HBN8, respectively.

states of carboxylic residues that are part of HBNs. In PSII, the HBNs identified herein raise a number of questions that can be addressed by theory and experiments in the foreseeable future: What are the pK_a values of the key titratable groups? Are protons delocalized in internal water cluster? How stable are the HBNs in MD simulations and what are the effects of mutating specific residues from the network? And most importantly, how do the HBN-facilitated protonation dynamics relate to the functioning of PSII? Aside from computational approaches, FTIR difference [82] and novel time-resolved IR experiments [83] may be especially well suited to address these questions.

5.3. A role for protonated carboxylate dyads in PSII?

If in physiological conditions the D2-E344/CP47-D380 dyad (Fig. 4E) harbors a proton in the form of a stable and barrier-less H bond [84] as the 2.6 Å crystal-structure distance between the carboxylates suggests (Table 1, Fig. 4E), the important question arises as to the functional significance of such a protonated carboxylate dyad. One possibility is that the carboxylate dyad is protonated throughout the reaction cycle, and it serves simply to glue together the D2 and CP47 subunits.

Alternatively, the H bond between D2-E344 and CP47-D380 may be present only at specific times along the reaction pathway. Changes in the electrostatic environment of the carboxylate dyad or protein conformational changes coupled to the OEC reactions could result in breaking of the D2-E344/CP47-D380 H-bond. Subsequent deprotonation of the carboxylate dyad and the resulting electrostatic repulsion between D2-E344 and CP47-D380 could lead to further, more extended conformational changes. In this scenario, when the D2-E344/CP47-D380 H-bond is broken, the negatively-charged D2-

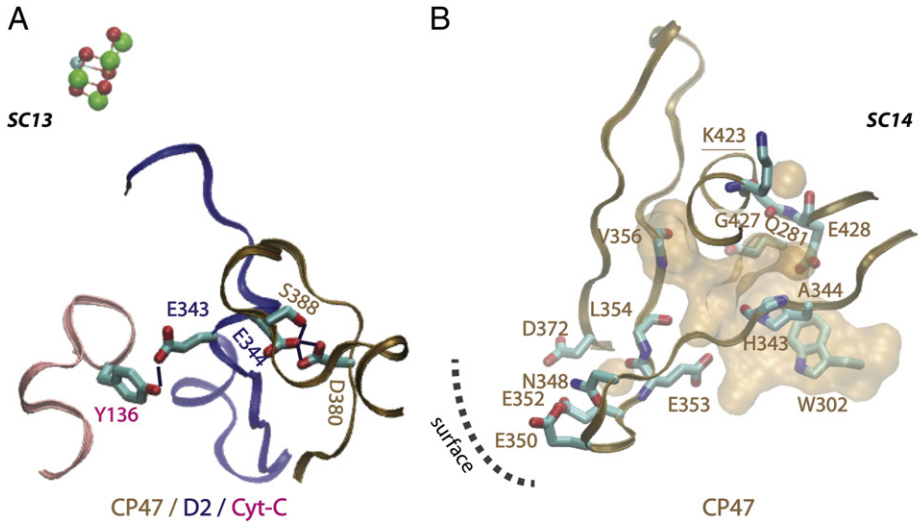

Fig. 10. Surface clusters can mediate tight inter-subunit interactions and shape hydrophilic pockets. (A) Tight inter-subunit interactions mediated by carboxylic amino acids in SC13. The carboxylic oxygen atoms of CP47-D380 are within 2.6–3.3 Å of D2-E344 (see the black lines connecting the carboxylic groups). Such a short distance suggests a strong, proton-sharing H-bond. One amino acid downstream E344 in the sequence of subunit D2, E343 hydrogen bonds to Y136 of the soluble Cyt-c (3.0 Å distance). That is, the E343/E344 segment of subunit D2 ensures coupling of subunit D2 with CP47 and Cyt-c. D2-E343 is also part of HBN2 (Fig. 7A). (B) A hydrophilic pocket on the surface of PSII (SC14). Residues E350, E352, and D372 of CP47 are located on the surface, at the entry towards a hydrophilic cavity filled with about 30 H-bonding water molecules. The water/protein HBN includes H-bonding (distance of 2.8 Å) between a water molecule and the K423 backbone. The sidechain of CP47-K423 is part of an HBN that includes amino acid residues from CP47, D2, and PsbO (see HBN11, Fig. 9E).

E344 can engage in other HBNs. We note that the discussion of the D2-E344/CP47-D380 dyad is highly speculative, aiming to illustrate how protonated carboxylate dyads could contribute to a dynamic control of PSII function.

In summary, the carboxylate dyads described herein may serve an exclusively structural role. However, an active role in proton management and relocation is also conceivable. Changes in the protein conformation that result in an increased distance between the two carboxylate groups could promote release of the protons previously harbored by the carboxylate dyad. Alternatively, protonation state changes could induce dyad dissolution and thereby major changes in the protein conformation.

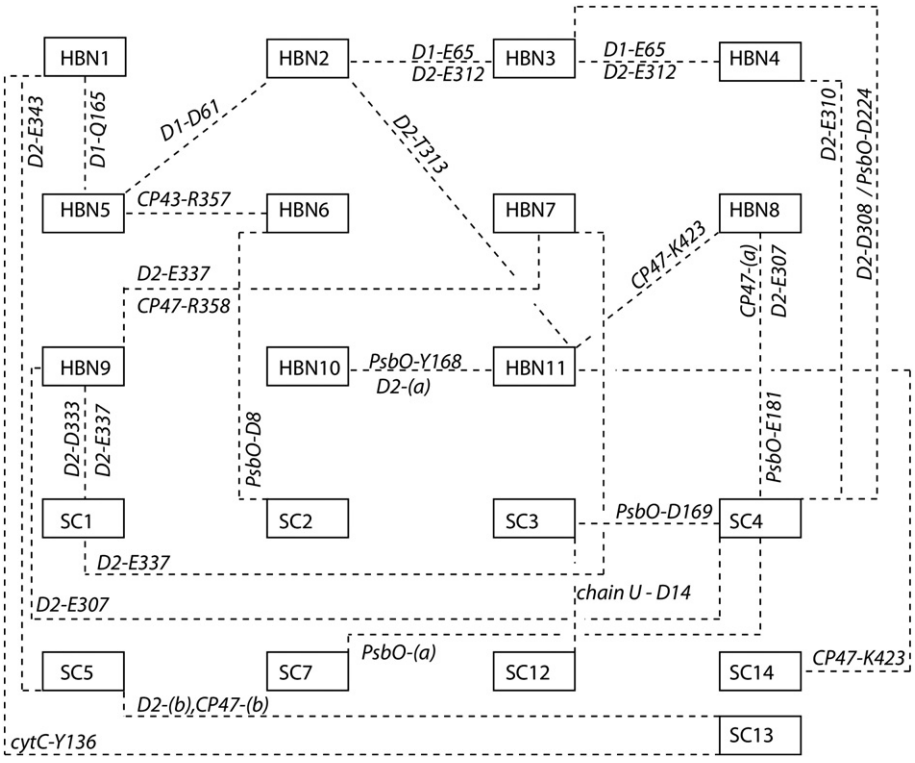

Fig. 11. Schematic representation of inter-connections between clusters and HBNs. Interconnections are indicated by dashed lines; examples of amino acids that are common to the corresponding clusters/HBNs are given for each pair. For details about the composition of the clusters and the HBNs, see Figs. 4–11. *D2-(a)*, *D2-(b)*, *PsbO-(a)*, and *CP47-(a)* include several connecting residues each, namely D2-E323, D2-R326, and D2-D207 (*D2-(a)*); D2-E343 and D2-E344 (*D2-(b)*); PsbO-D222 and PsbO-D224 (*PsbO-(a)*); CP47-D433 and CP47-E435; CP47-D372, CP47-E350, CP47-E352, and CP47-E353 (*CP47-(a)*).

Table 1
Pairs of carboxylic residue residues (AA1 paired with AA2) whose carboxylic groups are located within short, H-bonding distances.

AA1	AA2	Distance (Å)	Figures
PsbO-E97	PsbO-D102	2.8	5D
D2-E344	CP47-D380	2.6	4E, 10A
D1-E65	D2-E312	2.5	7B–D
CP47-E405	CP47-E431	2.6–3.7[a]	4D

[a] Distances measured for conformation-(1) of the CP47-E405 sidechain, taken as the shortest oxygen–oxygen distance between CP47-E405 and CP47-E431 in either of the E431 conformations (Fig. 4E). In the corresponding figures (indicated in the right column), the short distances are indicated by black lines connecting the oxygen atoms.

6. From OEC to lumenal surface: H-bonded networks for proton transfer and long-distance conformational coupling

6.1. HBNs that start at D1-Y161(Tyr_Z)

The presence of HBNs that start in the vicinity of the OEC has been considered before [19,43,46,2,8]. Umena et al. [2] noted an HBN that extends from D1-Y161 to PsbV-Y137/K129 via D1 residues H190, N298, H304, D319, N322, R323, and water molecules (Fig. 2C). This is a long, curved pathway that includes residues from four protein subunits, and reaches to the bulk via the flexible R55 of the Cyt-c subunit (Fig. 7A). The entrance site of the path is at the redox-active tyrosine (D1-Y161, also denoted as Tyr_Z or Y_Z, Fig. 1). In the H-atom abstraction model of Babcock and coworkers [85–87], it was assumed that deprotonation of D1-Y161 is followed by transfer of the phenolic proton to the lumenal bulk before transfer of an H-atom from the Mn_4Ca complex to the Y_Z radical. Whether or not HBN7 (Fig. 7A) indeed participates in proton removal from the OEC-site via the redox-active Tyr_Z (D1-Y161), in all or some of the S-state transitions of PSII, is an important open question. In the static picture provided by protein crystallography, the proton transfer path appears to be interrupted at the D1/D2 interface. A continuous proton transfer path leading from the OEC to the surface that may be established via relatively minor conformational changes is conceivable.

6.2. The CP43-R357 H-bonded networks

The sidechain of CP43-R357 is part of an HBN in the immediate vicinity of the OEC core (HBN5, Fig. 8A). A direct participation of CP43-R357 in proton translocation and water oxidation has been proposed from continuum electrostatic computations [47] and QM/MM modeling [88]. Site-directed mutagenesis of CP43-R357 severely impairs PSII function [89]. The CP43-R357 residue may represent the entrance site of an HBN that connects the OEC region to the bulk (HBN6, Fig. 8B). The backbone of CP43-R357 (but not its protonatable sidechain) connects to HBN6 that reaches to the bulk via PsbO-D8 (Fig. 8B). Conformational dynamics of residues or water molecules may be required for efficient proton transfer from HBN5 to HBN6. CP43-D360 appears to have a central role in HBN6, as it bridges to two water clusters that H-bond to protein sidechain and backbone groups (Figs. 3B, 8B).

6.3. H-bonding of the pivotal D1–D61 group

D1–D61 (Fig. 2C) is part of the putative proton-transfer channels discussed, e.g., by Ho [8]. Barber and coworkers [19] had noted that D1–D61 is at the mouth of a hydrophilic channel that extends from D1 to D2 and PsbO, and involves D1-E65, D2-E312, and additional polar groups. The participation of D1-E65 (Fig. 2C) in a hydrophilic channel was confirmed by a recent search for channels in PSII [46] based on the 2.9 Å-resolution crystal structure from [90] and ultimately by the 1.9 Å crystallographic model of Shen et al. [2]. In the D1–D61N mutant, electron transfer and likely also proton transfer have been found to be drastically slowed down [91,92].

The D1–D61 is part of an extended HBN comprised by protein groups and water molecules. Via D1-E65/D2-E312 and water molecules, D61 connects to a polar H-bonded cluster contributed by amino acids from subunits D1 and D2 (Fig. 7B): A water molecule bridges to D2-E312 and D2-T316 via H-bonding (distance of 2.8 Å, HBN2 in Fig. 7B). The hydroxyl group of D2-T316 H-bonds to the amide group of D2-T313, and the D2-T313 hydroxyl is part of a H-bonded cluster that comprises D2-Q301 and D1 groups G74, N75, N76, and T79 (Fig. 7B). The role of this intriguing network of Asn/Gln/Thr H-bonds is not clear. In membrane proteins, clusters of H bonds composed of three amino acid residues on two different transmembrane helices (so called polar clamps) were proposed to provide structural constraints for the helices [93]. We suggest that the Asn/Gln/Thr cluster in HBN2 may play a similar role, serving as a node of tight interactions between subunits D1 and D2.

6.4. Branched water wires starting at the D1-E65/D2-E312 dyad

Detailed inspection of the crystal structure of Umena et al. [2] reveals that the carboxylic groups of D1-E65 and D2-E312 are within a short distance of 2.5 Å (Fig. 7B, Table 1); such a short distance would indicate a proton-carrying carboxylate dyad (see Section 5). The D1-E65/D2-E312 dyad further communicates with the network of water wires depicted in Fig. 7C and D, with HBN11 via D2-T313 (Fig. 9E), and with SC4 via PsbO-D224 (Fig. 4D); that is, the protein/water network involving the D1-E65/D2-E312 dyad extends from the D61 region (Fig. 7B) towards the lumen.

The network of water wires close to the D1-E65/D2-E312 dyad could be described as a main wire extending from D1-E65 to D1-Y73 (orange line in Fig. 7C) that branches out into three wires (see the cyan, gray, and dark yellow transparent surfaces), with an additional branch in the vicinity of D2-E310 (see the ice blue surface in Fig. 7D). The water wires can lead to backbone groups (e.g., the cyan wire ends at the PsbO-F156/PsbO-L164 backbone), or to titratable protein groups that could be involved in proton transfer (e.g., D2-E310, D2-D308, or PsbO-D224). The D2 amino acids D308 and E310 are close to the surface, where they are part of a network of H bonds involving water molecules and PsbO groups (SC4 in Fig. 4D).

The D1-E65/D2-E312 network appears to have extensive connections throughout PSII. D2-T313 is close to a cluster of hydrophilic groups contributed by subunits D2, CP47, and PsbO, including the sidechain of CP47-K423 (Fig. 9E). The backbone of CP47-K423 participates in stabilizing a water network on the surface of CP47 (Fig. 10B). The finding that D1-E65 and D2-E312 are part of an extensive protein/water HBN that has interconnections extending to the lumen is compatible with results obtained by FTIR difference spectroscopy supporting the idea of a proton excess channel that includes D1–D61, D1-E65, and D2-E312, and links the OEC with the lumen (Service et al. [82]).

7. Extended H-bonded networks connecting protein subunits

7.1. Examples of HBNs interconnecting subunits

The subunits of PSII are inter-connected via networks of H bonds formed by protein groups and water molecules. The D2 subunit has extensive couplings to other subunits: D2 groups participate in clusters of hydrophilic residues with groups from D1 (Fig. 7), CP43 (Fig. 8A), CP47 (Figs. 9, 4A, D, and E), PsbO (Fig. 4D), and Cyt-c, (Figs. 7A, 10A), and PsbH (HBN7, Fig. 9A).

The region in the D2 sequence comprising E343 and E344 connects via H-bonding to both CP47 and Cyt-c (Figs. 4E, 10A). D2 further connects to PsbO via the H bond between PsbO-Y168 and D2-E323 in HBN10 (Fig. 9D). D2-E323 also is part of the crowded cluster depicted in Fig. 9E

(HBN11) that couples back to the D1-E65/D2-E312 dyad (HBN2, Fig. 7B): D2-T313 H bonds with D2-Q301 in HBN2 (Fig. 7B); in HBN11, D2-T313 H bonds to the D2-Y315 backbone (Fig. 9E). The sidechain of D2-Y315 H bonds to D2-E302, which in turn H-bonds to PsbO-K160.

CP47-E364 is at the heart of an extensive coupling between D2 and CP47 (see HBN10 in Fig. 9D): The carboxyl oxygen atoms of CP47-E364 are within H-bonding distance from D2-R294 and CP47-R326 (2.8–2.9 Å distances). CP47-R326 has the potential to H bond to D2-D297 (3.7 Å distance). On the other side of the CP47-E364 carboxyl group, D2-R294 further H bonds to D2-H189 (3.5 Å distance), and H189 to D2-Y160 (2.7 Å distance). D2-Y160 contributes to a protein/water network in HBN9 that effectively bridges D2-Y160 (and the groups to which it H bonds in HBN10) to a network of protein/water H bonds reaching to CP47-R357 (Fig. 9C): D2-Y160 bridges via water and D2-R180 to D2-D333, which is part of the protein/water HBN leading to CP47-R357 via D2-Q334 and D2-E337. D2 groups D333 and E337 are part of the protein/water cluster bridging D2 and CP47 at the surface (Fig. 4A).

7.2. Possible role of interconnecting HBNs in conformational and protonation dynamics

The HBNs discussed here were identified by analyzing a static crystal structure. In a physiological environment, the H bonds in the crowded clusters and networks will likely exhibit complex dynamics: within one cluster, specific H bonds may be stable, whereas others break and reform on various timescales. Indeed, complex patterns of H-bond dynamics have been observed in MD simulations of the SecYEG protein translocon, a protein with numerous clusters of H bonds [94].

Dynamic H bonds can ensure an efficient mechanism of long-distance intra-protein coupling; such a coupling can facilitate rapid propagation of conformational changes [95]. For example, release of the proton from the putative D1-E65/D2-E312 network (Fig. 7B–D) would affect the local structure of subunits D1, D2, and PsbO that contribute to the network. Breaking of the strong H bonds between D2-E344 and CP47-D380 (Fig. 10A) could imply enhanced dynamics of D2 and CP47, which would in turn affect the dynamics of the D2 and CP47 HBNs. That is, the inter-subunit HBNs could not only contribute structural stability, but may also ensure a tight long-distance coupling between the protonation state and protein conformation.

Experimental data on the functional role of inter-subunit interactions are rather limited. An observation that may support an important role of inter-subunit H bonds is the 50% reduction in the steady-state oxygen evolution in the spinach D2-E303V (D2-E302 in *T. vulcanus*) PSII mutant; the mutagenesis effect was interpreted to suggest a role of D2-E303 in stabilizing D2/PsbO interactions [96]. D2-E302 is part of a protein/water HBN (HBN11 in Fig. 9E) that connects, via D2-T313, deep into the PS-II OEC region at the D1-E65/D2-E312 region (HBN2, Fig. 7B).

The presence of carboxylate clusters at the interface between several PSII subunits (Fig. 4) could lead to different strengths of the inter-subunit interactions depending on the solution pH; given that some of the surface carboxylate clusters couple with regions close to the OEC, changes in the external pH could be relayed to the OEC region. The extensive coupling between various regions of PSII (Fig. 11) suggests that coupling between some of surface clusters to more internal groups close to the OEC could also lead to the dynamics of the surface-carboxylate/water networks being influenced by the chemical reactions and structural changes associated with the reaction cycle. The inter-subunit couplings throughout PSII may also be essential for the assembly of the PSII complex, and for its structural stability. The observation that the D1 subunit is exchanged in the course of the PSII repair cycle (for review see [97,4,6,98]) suggests that the strength of the inter-subunit HBNs may be fine-tuned to provide the right balance between structural stability and flexibility: the inter-subunit H bonds of D2 must be strong enough to maintain the overall integrity of PSII, but break when an impaired D2 is replaced.

8. Conclusions

Based on the recent crystallographic model of Umena et al. [2], we searched for HBNs in the lumenal region of PSII. We found extended HBNs that involve protein groups and water molecules. At the surface of PSII there are numerous carboxylate clusters that are expected to form HBNs with water molecules of the aqueous electrolyte. The HBNs and carboxylate/water clusters also contain groups that are not H-bonded in the crystal structure, but could easily H-bond at least transiently because of molecular dynamics. The remarkable network of intra- and inter-subunit interactions in PSII (Figs. 3–11) suggests a tight coupling between distant regions of PSII via extended and interconnected HBNs. In the dark, such a coupling may ensure stability of the protein conformation. In the light-driven reactions, the extensive HBNs discussed here could ensure a rapid and efficient coupling between proton transfer reactions and protein conformation. This role of the HBNs is supported by observations in the SecYEG protein translocon: extensive H-bond networks that interconnect different regions of the translocon make the closed-state geometry rather rigid, and ensure rapid long-distance propagation of conformational changes [94].

Several pairs of carboxylic groups were found within short distances that suggest H-bonding or even proton sharing in the form of a barrierless H bond (Table 1). The D1-E65/D2-E312 dyad is an especially intriguing example, because this dyad communicates with a complex network of protein/water H-bonds extending from the D1–D61 region (Fig. 7 B) towards PsbO (Fig. 7C and D). The D1-E65/D2-E312 HBNs are also coupled to other regions of PSII (Fig. 7C–D, Fig. 11). Experimental results on the role of this carboxylate dyad are still scarce. Recent FTIR difference spectroscopy data [82] were interpreted to suggest that D1-E65 and D2-E312 are part of a protein/water HBN that includes a protonated carboxylate whose pK_a (and thus protonation state) changes during the $S_1 \rightarrow S_2$ transition. Pursuant to the FTIR data, we suggest that the D1-E65–D2-E312 dyad may undergo protonation/deprotonation reactions during the reaction cycle and that changes in the protonation state of the dyad carboxylates are coupled to protein conformational changes.

The D1-E65/D2-E312 HBN communicates with PsbO amino acids that are part of surface inter-subunit and intra-subunit carboxylate/water clusters (Figs. 7C, 4D, 5C). The carboxylate/water surface clusters could be associated with paths for the propagation of protons [65] or with controlling the local structure and dynamics of the protein. Their presence and dynamics likely depend on the pH. The extensive coupling between various regions of PSII suggests that the dynamics of the surface-carboxylate/water networks could be influenced by the chemical reactions and structural changes associated with the reaction cycle of water-oxidation.

Our assessment of the extended H-bonded networks in the protein interior and of the truly remarkable carboxylate clusters represents a first step towards understanding of their functional role. The tentative identification of key groups may stimulate their investigation by site-directed mutagenesis in conjunction with advanced biophysical characterization and computational approaches. (However, the extensive couplings via H bonds highlight the need of caution in interpreting the molecular origin of the site-directed mutagenesis effects.) Especially our discussion of the functional role of HBNs and surface clusters is, at present, largely speculative. Numerous general and specific questions are awaiting clarification by future experimental and computational investigations.

Acknowledgements

We thank Dr. Ivelina Zaharieva (FU Berlin) for assistance with Fig. 1. HD acknowledges financial support by the Bundesministerium für Bildung und Forschung (BMBF, "H_2 design cell" consortium) and the European Union (7th framework program, SOLAR-H2 consortium). A-NB

is supported in part by the Marie Curie International Reintegration Grant (FP7-PEOPLE-2010-RG 276920).

References

[1] J. Barber, Photosynthetic energy conversion: natural and artificial, Chem. Soc. Rev. 38 (2009) 185–196.
[2] Y. Umena, K. Kawakami, J.-R. Shen, N. Kamiya, Crystal structure of oxygen-evolving photosystem II at a resolution of 1.9 Å, Nature 473 (2011) 55–60.
[3] T.M. Bricker, J.L. Roose, R.D. Fagerlund, L.K. Frankel, J.J. Eaton-Rye, The extrinsic proteins of Photosystem II, Biochim. Biophys. Acta 1817 (2012) 121–142.
[4] D.A. Campbell, E. Tyystjarvi, Parameterization of photosystem II photoinactivation and repair, Biochim. Biophys. Acta 1817 (2012) 258–265.
[5] T. Cardona, A. Sedoud, N. Cox, A.W. Rutherford, Charge separation in photosystem II: a comparative and evolutionary overview, Biochim. Biophys. Acta 1817 (2012) 26–43.
[6] W. Chi, X. Sun, L. Zhang, The roles of chloroplast proteases in the biogenesis and maintenance of photosystem II, Biochim. Biophys. Acta 1817 (2012) 239–246.
[7] A. Grundmeier, H. Dau, Structural models of the manganese complex of photosystem II and mechanistic implications, Biochim. Biophys. Acta 1817 (2012) 88–105.
[8] F.M. Ho, Structural and mechanistic investigations of photosystem II through computational methods, Biochim. Biophys. Acta 1817 (2012) 106–120.
[9] R. Kouril, J.P. Dekker, E.J. Boekema, Supramolecular organization of photosystem II in green plants, Biochim. Biophys. Acta 1817 (2012) 2–12.
[10] N. Mizusawa, H. Wada, The role of lipids in photosystem II, Biochim. Biophys. Acta 1817 (2012) 194–208.
[11] F. Muh, C. Glockner, J. Hellmich, A. Zouni, Light-induced quinone reduction in photosystem II, Biochim. Biophys. Acta 1817 (2012) 44–65.
[12] P. Mulo, I. Sakurai, E.M. Aro, Strategies for psbA gene expression in cyanobacteria, green algae and higher plants: from transcription to PSII repair, Biochim. Biophys. Acta 1817 (2012) 247–257.
[13] P. Pospisil, Molecular mechanisms of production and scavenging of reactive oxygen species by photosystem II, Biochim. Biophys. Acta 1817 (2012) 218–231.
[14] L.X. Shi, M. Hall, C. Funk, W.P. Schroder, Photosystem II, a growing complex: updates on newly discovered components and low molecular mass proteins, Biochim. Biophys. Acta 1817 (2012) 13–25.
[15] K.E. Shinopoulos, G.W. Brudvig, Cytochrome b and cyclic electron transfer within photosystem II, Biochim. Biophys. Acta 1817 (2012) 66–75.
[16] S. Styring, J. Sjöholm, F. Mamedov, Two tyrosines that changed the world: Interfacing the oxidizing power of photochemistry to water splitting in photosystem II, Biochim. Biophys. Acta 1817 (2012) 76–87.
[17] I. Vass, Molecular mechanisms of photodamage in the Photosystem II complex, Biochim. Biophys. Acta 1817 (2012) 209–217.
[18] A. Zouni, H.T. Witt, J. Kern, P. Fromme, N. Krauss, W. Saenger, P. Orth, Crystal structure of photosystem II from *Synechococcus elongatus* at 3.8 Å resolution, Nature 409 (2001) 739–743.
[19] K.N. Ferreira, T.M. Iverson, K. Maghlaoui, J. Barber, S. Iwata, Architecture of the photosynthetic oxygen-evolving center, Science 303 (2004) 1831–1838.
[20] F. Rappaport, B.A. Diner, Primary photochemistry and energetics leading to the oxidation of the $(Mn)_4Ca$ cluster and to the evolution of molecular oxygen in Photosystem II, Coord. Chem. Rev. 252 (2008) 259–272.
[21] H. Dau, I. Zaharieva, Principles, efficiency, and blueprint character of solar-energy conversion in photosynthetic water oxidation, Acc. Chem. Res. 42 (2009) 1861–1870.
[22] M. Haumann, P. Liebisch, C. Muller, M. Barra, M. Grabolle, H. Dau, Photosynthetic O_2 formation tracked by time-resolved X-ray experiments, Science 310 (2005) 1019–1021.
[23] H. Dau, M. Haumann, Reaction cycle of photosynthetic water oxidation in plants and cyanobacteria (response letter), Science 312 (2006) 1471–1472.
[24] J. Buchta, M. Grabolle, H. Dau, Photosynthetic dioxygen formation studied by time-resolved delayed fluorescence measurements—method, rationale, and results on the activation energy of dioxygen formation, Biochim. Biophys. Acta 1767 (2007) 565–574.
[25] H. Dau, M. Haumann, Time-resolved X-ray spectroscopy leads to an extension of the classical S-state cycle model of photosynthetic oxygen evolution, Photosynth. Res. 92 (2007) 327–343.
[26] L. Gerencser, H. Dau, Water oxidation by photosystem II: H2O−D2O exchange and the influence of pH support formation of an intermediate by removal of a proton before dioxygen creation, Biochemistry 49 (2010) 10098–10106.
[27] P. Chernev, I. Zaharieva, H. Dau, M. Haumann, Carboxylate shifts steer inter-quinone electron transfer in photosynthesis, J. Biol. Chem. 286 (2011) 5368–5374.
[28] F. Rappaport, N. Ishida, M. Sugiura, A. Boussac, Ca^{2+} determines the entropy changes associated with the formation of transition states during water oxidation by Photosystem II, Energy Environ. Sci. 4 (2011) 2520–2524.
[29] I. Zaharieva, J.M. Wichmann, H. Dau, Thermodynamic limitations of photosynthetic water oxidation at high proton concentrations, J. Biol. Chem. 286 (2011) 18222–18228.
[30] H. Dau, M. Haumann, Eight steps preceding O–O bond formation in oxygenic photosynthesis—a basic reaction cycle of the photosystem II manganese complex, Biochim. Biophys. Acta 1767 (2007) 472–483.
[31] H. Dau, M. Haumann, The manganese complex of photosystem II in its reaction cycle—basic framework and possible realization at the atomic level, Coord. Chem. Rev. 252 (2008) 273–295.
[32] F.M. Ho, Uncovering channels in photosystem II by computer modelling: current progress, future prospects, and lessons from analogous systems, Photosynth. Res. 98 (2008) 503–522.
[33] E.M. Sproviero, J.A. Gascon, J.P. McEvoy, G.W. Brudvig, V.S. Batista, Computational studies of the O_2-evolving complex of photosystem II and biomimetic oxomanganese complexes, Coord. Chem. Rev. 252 (2008) 395–415.
[34] H. Dau, P. Liebisch, M. Haumann, The structure of the manganese complex of photosystem II in its dark-stable S_1-state: EXAFS results in relation to recent crystallographic data, Phys. Chem. Chem. Phys. 6 (2004) 4781–4792.
[35] J. Yano, J. Kern, K.-D. Irrgang, M.J. Latimer, U. Bergmann, P. Glatzel, Y. Pushkar, J. Biesiadka, B. Loll, K. Sauer, J. Messinger, A. Zouni, V.K. Yachandra, X-ray damage to the Mn_4Ca complex in single crystals of photosystem II: a case study for metalloprotein crystallography, Proc. Natl. Acad. Sci. U. S. A. 102 (2005) 12047–12052.
[36] M. Grabolle, M. Haumann, C. Müller, P. Liebisch, H. Dau, Rapid loss of structural motifs in the manganese complex of oxygenic photosynthesis by X-ray irradiation at 10–300 K, J. Biol. Chem. 281 (2006) 4580–4588.
[37] B. Kok, B. Forbush, M. McGloin, Cooperation of charges in photosynthetic O_2 evolution — I. A linear four-step mechanism, Photochem. Photobiol. 11 (1970) 457–475.
[38] J.P. McEvoy, G.W. Brudvig, Water-splitting chemistry of photosystem II, Chem. Rev. 106 (2006) 4455–4483.
[39] W. Junge, M. Haumann, R. Ahlbrink, A. Mulkidjanian, J. Clausen, Electrostatics and proton transfer in photosynthetic water oxidation, Phil. Trans. R. Soc. B 357 (2002) 1407–1418.
[40] R.E. Blankenship, Molecular Mechanisms of Photosynthesis, Blackwell Science, Oxford, England, 2002.
[41] D.M. Kramer, J.A. Cruz, A. Kanazawa, Balancing the central roles of the thylakoid proton gradient, Trends Plant Sci. 8 (2003) 27–32.
[42] S. Vasil'ev, D. Bruce, A protein dynamics study of photosystem II: the effects of protein conformation on reaction center function, Biophys. J. 90 (2006) 3062–3073.
[43] J.W. Murray, J. Barber, Structural characteristics of channels and pathways in photosystem II including the identification of an oxygen channel, J. Struct. Biol. 159 (2007) 228–237.
[44] S. Vassiliev, P. Comte, A. Mahboob, D. Bruce, Tracking the flow of water through photosystem II using molecular dynamics and streamline tracing, Biochemistry 49 (2010) 1873–1881.
[45] W. Humphrey, A. Dalke, K. Schulten, VMD: visual molecular dynamics, J. Mol. Graph. 14 (1996) 33–8, 27–8.
[46] A. Gabdulkhakov, A. Guskov, M. Broser, J. Kern, F. Muh, W. Saenger, A. Zouni, Probing the accessibility of the Mn(4)Ca cluster in photosystem II: channels calculation, noble gas derivatization, and cocrystallization with DMSO, Structure 17 (2009) 1223–1234.
[47] H. Ishikita, E.W. Knapp, Function of redox-active tyrosine in photosystem II, Biophys. J. 90 (2006) 3886–3896.
[48] F.M. Ho, S. Styring, Access channels and methanol binding site to the CaMn4 cluster in Photosystem II based on solvent accessibility simulations, with implications for substrate water access, Biochim. Biophys. Acta 1777 (2008) 140–153.
[49] J.A. Hanson, K. Duderstadt, L.P. Watkins, S. Bhattacharyya, J. Brokaw, J.W. Chu, H. Yang, Illuminating the mechanistic roles of enzyme conformational dynamics, Proc. Natl. Acad. Sci. U. S. A. 104 (2007) 18055–18060.
[50] K.A. Henzler-Wildman, M. Lei, V. Thai, S.J. Kerns, M. Karplus, D. Kern, A hierarchy of timescales in protein dynamics is linked to enzyme catalysis, Nature 450 (2007) 913–916.
[51] J. Köfinger, G. Hummer, C. Dellago, Single-water in nanopores, Phys. Chem. Chem. Phys. 13 (2011) 15403–15417.
[52] R.A. Capaldi, G. Vanderkooi, The low polarity of many membrane proteins, Proc. Natl. Acad. Sci. U. S. A. 69 (1972) 930–932.
[53] D. Oesterhelt, W. Stoeckenius, Functions of a new photoreceptor membrane, Proc. Natl. Acad. Sci. U. S. A. 70 (1973) 2853–2857.
[54] R. Mitchell, P.R. Rich, Proton uptake by cytochrome c oxidase on reduction and on ligand binding, Biochim. Biophys. Acta 1186 (1994) 19–26.
[55] R.M. Nyquist, D. Heitbrink, C. Bolwien, R.B. Gennis, J. Heberle, Direct observation of protonation reactions during the catalytic cycle of cytochrome c oxidase, Proc. Natl. Acad. Sci. U. S. A. 100 (2003) 8715–8720.
[56] I. Belevich, M.I. Verkhovsky, M. Wikstrom, Proton-coupled electron transfer drives the proton pump of cytochrome c oxidase, Nature 440 (2006) 829–832.
[57] T. Shutova, V.V. Klimov, B. Andersson, G. Samuelsson, A cluster of carboxylic groups in PsbO protein is involved in proton transfer from the water oxidizing complex of Photosystem II, Biochim. Biophys. Acta 1767 (2007) 434–440.
[58] H. Popelkova, A. Commet, C.F. Yocum, Asp157 is required for the function of PsbO, the photosystem II manganese stabilizing protein, Biochemistry 48 (2009) 11920–11928.
[59] J.R. Shen, M. Qian, Y. Inoue, R.L. Burnap, Functional characterization of *Synechocystis* sp. PCC 6803 delta psbU and delta psbV mutants reveals important roles of cytochrome c-550 in cyanobacterial oxygen evolution, Biochemistry 37 (1998) 1551–1558.
[60] R.S. Hutchison, J.J. Steenhuis, C.F. Yocum, M.R. Razeghifard, B.A. Barry, Deprotonation of the 33-kDa, extrinsic, manganese-stabilizing subunit accompanies photooxidation of manganese in photosystem II, J. Biol. Chem. 274 (1999) 31987–31995.
[61] R.K. Sachs, K.M. Halverson, B.A. Barry, Specific isotopic labeling and photooxidation-linked structural changes in the manganese-stabilizing subunit of photosystem II, J. Biol. Chem. 278 (2003) 44222–44229.
[62] T. Shutova, J. Nikitina, G. Deikus, B. Andersson, V. Klimov, G. Samuelsson, Structural dynamics of the manganese-stabilizing protein-effect of pH, calcium, and manganese, Biochemistry 44 (2005) 15182–15192.

[63] Y. Marantz, E. Nachliel, A. Aagaard, P. Brzezinski, M. Gutman, The proton collecting function of the inner surface of cytochrome c oxidase from Rhodobacter sphaeroides, Proc. Natl. Acad. Sci. U. S. A. 95 (1998) 8590–8595.
[64] V. Sacks, Y. Marantz, A. Aagard, S. Checover, E. Nachliel, M. Gutman, The dynamic feature of the proton collecting antenna of a protein surface, Biochim. Biophys. Acta 1365 (1998) 232–240.
[65] M. Gutman, E. Nachliel, R. Friedman, The mechanism of proton transfer between adjacent sites on the molecular surface, Biochim. Biophys. Acta 1757 (2006) 931–941.
[66] R. Friedman, E. Nachliel, M. Gutman, Molecular dynamics of a protein surface: ion-residues interactions, Biophys. J. 89 (2005) 768–781.
[67] S. Checover, E. Nachliel, N.A. Dencher, M. Gutman, Mechanism of proton entry into the cytoplasmic section of the proton-conducting channel of bacteriorhodopsin, Biochemistry 36 (1997) 13919–13928.
[68] H. Yu, I.M. Ratheal, P. Artigas, B. Roux, Protonation of key acidic residues is critical for the K-selectivity of the Na/K pump, Nat. Struct. Mol. Biol. 18 (2011) 1159–1163.
[69] A.-N. Bondar, J.C. Smith, Water molecules in short- and long-distance proton transfer steps of bacteriorhodopsin proton pumping, Isr. J. Chem. 49 (2009) 155–161.
[70] P. Goyal, N. Ghosh, P. Phatak, M. Clemens, M. Gaus, M. Elstner, Q. Cui, Proton storage site in bacteriorhodopsin: new insights from quantum mechanics/molecular mechanics simulations of microscopic pK(a) and infrared spectra, J. Am. Chem. Soc. 133 (2011) 14981–14997.
[71] J.P. Morth, B.P. Pedersen, M.S. Toustrup-Jensen, T.L. Sorensen, J. Petersen, J.P. Andersen, B. Vilsen, P. Nissen, Crystal structure of the sodium–potassium pump, Nature 450 (2007) 1043–1049.
[72] T. Shinoda, H. Ogawa, F. Cornelius, C. Toyoshima, Crystal structure of the sodium–potassium pump at 2.4 A resolution, Nature 459 (2009) 446–450.
[73] H. Luecke, B. Schobert, H.T. Richter, J.P. Cartailler, J.K. Lanyi, Structure of bacteriorhodopsin at 1.55 A resolution, J. Mol. Biol. 291 (1999) 899–911.
[74] L.S. Brown, J. Sasaki, H. Kandori, A. Maeda, R. Needleman, J.K. Lanyi, Glutamic acid 204 is the terminal proton release group at the extracellular surface of bacteriorhodopsin, J. Biol. Chem. 270 (1995) 27122–27126.
[75] A.K. Dioumaev, H.T. Richter, L.S. Brown, M. Tanio, S. Tuzi, H. Saito, Y. Kimura, R. Needleman, J.K. Lanyi, Existence of a proton transfer chain in bacteriorhodopsin: participation of Glu-194 in the release of protons to the extracellular surface, Biochemistry 37 (1998) 2496–2506.
[76] L. Essen, R. Siegert, W.D. Lehmann, D. Oesterhelt, Lipid patches in membrane protein oligomers: crystal structure of the bacteriorhodopsin-lipid complex, Proc. Natl. Acad. Sci. U. S. A. 95 (1998) 11673–11678.
[77] C. Zscherp, J. Schlessinger, J. Tittor, D. Oesterhelt, J. Heberle, In situ determination of transient pKa changes of internal amino acids of bacteriorhodopsin by using time-resolved attenuated total reflection Fourier-transform infrared spectroscopy, Proc. Natl. Acad. Sci. U. S. A. 96 (1999) 5498–5503.
[78] R. Rousseau, V. Kleinschmidt, U.W. Schmitt, D. Marx, Assigning protonation patterns in water networks in bacteriorhodopsin based on computed IR spectra, Angew. Chem. Int. Ed. Engl. 43 (2004) 4804–4807.
[79] F. Garczarek, L.S. Brown, J.K. Lanyi, K. Gerwert, Proton binding within a membrane protein by a protonated water cluster, Proc. Natl. Acad. Sci. U. S. A. 102 (2005) 3633–3638.
[80] F. Garczarek, K. Gerwert, Functional waters in intraprotein proton transfer monitored by FTIR difference spectroscopy, Nature 439 (2006) 109–112.
[81] I.V. Kalaidzidis, I.N. Belevich, A.D. Kaulen, Photovoltage evidence that Glu-204 is the intermediate proton donor rather than the terminal proton release group in bacteriorhodopsin, FEBS Lett. 434 (1998) 197–200.
[82] R.J. Service, W. Hillier, R.J. Debus, Evidence from FTIR difference spectroscopy of an extensive network of hydrogen bonds near the oxygen-evolving Mn(4)Ca cluster of photosystem II involving D1-Glu65, D2-Glu312, and D1-Glu329, Biochemistry 49 (2010) 6655–6669.
[83] B.A. Barry, I.B. Cooper, A. De Riso, S.H. Brewer, D.M. Vu, R.B. Dyer, Time-resolved vibrational spectroscopy detects protein-based intermediates in the photosynthetic oxygen-evolving cycle, Proc. Natl. Acad. Sci. U.S.A. 103 (2006) 7288–7291.
[84] C.L. Perrin, J.B. Nielson, "Strong" hydrogen bonds in chemistry and biology, Annu. Rev. Phys. Chem. 48 (1997) 511–544.
[85] C.W. Hoganson, N. Lydakis-Simantiris, X.S. Tang, C. Tommos, K. Warncke, G.T. Babcock, B.A. Diner, J. McCracken, S. Styring, A hydrogen-atom abstraction model for the function of Y_Z in photosynthetic oxygen-evolution, Photosynth. Res. 46 (1995) 177–184.
[86] C.W. Hoganson, G.T. Babcock, A metalloradical mechanism for the generation of oxygen from water in photosynthesis, Science 277 (1997) 1953–1956.
[87] C. Tommos, G.T. Babcock, Oxygen production in nature: a light-driven metalloradical enzyme process, Acc. Chem. Res. 31 (1998) 18–25.
[88] E.M. Sproviero, J.A. Gascon, J.P. McEvoy, G.W. Brudvig, V.S. Batista, Quantum mechanics/molecular mechanics study of the catalytic cycle of water splitting in photosystem II, J. Am. Chem. Soc. 130 (2008) 3428–3442.
[89] H.J. Hwang, P. Dilbeck, R.J. Debus, R.L. Burnap, Mutation of arginine 357 of the CP43 protein of photosystem II severely impairs the catalytic S-state cycle of the H2O oxidation complex, Biochemistry 46 (2007) 11987–11997.
[90] A. Guskov, J. Kern, A. Gabdulkhakov, M. Broser, A. Zouni, W. Saenger, Cyanobacterial photosystem II at 2.9-Å resolution and the role of quinones, lipids, channels and chloride, Nat. Struct. Mol. Biol. 16 (2009) 334–342.
[91] M. Hundelt, A.M. Hays, R.J. Debus, W. Junge, Oxygenic photosystem II: the mutation D1–D61N in *Synechocystis* sp. PCC 6803 retards S-state transitions without affecting electron transfer from YZ to P680+, Biochemistry 37 (1998) 14450–14456.
[92] P.L. Dilbeck, H.J. Hwang, I. Zaharieva, L. Gerencser, H. Dau, R.L. Burnap, The mutation D1–D61N in *Synechocystis* sp. PCC 6803 allows the observation of pH-sensitive intermediates in the formation and release of O_2 from Photosystem II, Biochemistry 51 (2012) 1079–1091.
[93] L. Adamian, J. Liang, Interhelical hydrogen bonds and spatial motifs in membrane proteins: polar clamps and serine zippers, Proteins 47 (2002) 209–218.
[94] A.N. Bondar, C. del Val, J.A. Freites, D.J. Tobias, S.H. White, Dynamics of SecY translocons with translocation-defective mutations, Structure 18 (2010) 847–857.
[95] A.-N. Bondar, S.H. White, Hydrogen-bond dynamics in membrane protein function, Biochim Biophys. Acta 1818 (2012) 942–950.
[96] S. Rexroth, C.C. Wong, J.H. Park, J.R. Yates III, B.A. Barry, An activated glutamate residue identified in photosystem II at the interface between the manganese-stabilizing subunit and the D2 polypeptide, J. Biol. Chem. 282 (2007) 27802–27809.
[97] A. Rokka, M. Suorsa, A. Saleem, N. Battchikova, E.M. Aro, Synthesis and assembly of thylakoid protein complexes: multiple assembly steps of photosystem II, Biochem. J. 388 (2005) 159–168.
[98] M. Tikkanen, E.M. Aro, Thylakoid protein phosphorylation in dynamic regulation of photosystem II in higher plants, Biochim. Biophys. Acta 1817 (2012) 232–238.